A Mechanism for Nuclear Positioning in Fission Yeast Based on Microtubule Pushing✪

P.T. Tran,* L. Marsh,‡ V. Doye,§ S. Inoué,‖ and F. Chang*

*Department of Microbiology, Columbia University, New York, New York 10032; ‡Long Island University, Department of Biology, Brooklyn, New York 11201; §Institut Curie, Paris, Cedex 75005, France; and ‖Marine Biological Laboratory, Woods Hole, Massachusetts 02543

Abstract. The correct positioning of the nucleus is often important in defining the spatial organization of the cell, for example, in determining the cell division plane. In interphase *Schizosaccharomyces pombe* cells, the nucleus is positioned in the middle of the cylindrical cell in an active microtubule (MT)-dependent process. Here, we used green fluorescent protein markers to examine the dynamics of MTs, spindle pole body, and the nuclear envelope in living cells. We find that interphase MTs are organized in three to four antiparallel MT bundles arranged along the long axis of the cell, with MT plus ends facing both the cell tips and minus ends near the middle of the cell. The MT bundles are organized from medial MT-organizing centers that may function as nuclear attachment sites. When MTs grow to the cell tips, they exert transient forces produced by plus end MT polymerization that push the nucleus. After an average of 1.5 min of growth at the cell tip, MT plus ends exhibit catastrophe and shrink back to the nuclear region before growing back to the cell tip. Computer modeling suggests that a balance of these pushing MT forces can provide a mechanism to position the nucleus at the middle of the cell.

Key words: nuclear positioning • microtubule dynamics • microtubule-organizing center • green fluorescent protein • *Schizosaccharomyces pombe*

Introduction

Spatial organization of the cell requires that cells be able to measure distances, sense their size, and define their middles in order to position structures properly within the cell. In the establishment of cellular architecture, the positioning of the nucleus and its associated centrosome is especially important. Movements of the nucleus have been shown to play key roles during development, mitosis, and fertilization (Reinsch and Gonczy, 1998). Nuclear positioning is generally dependent on microtubules (MTs),[1] which are rigid dynamic polymers of αβ-tubulin (Inoué and Salmon, 1995; Desai and Mitchison, 1997) and an associated MT-organizing center (MTOC). MTs have been proposed to contribute to nuclear movement in a least three ways (see Reinsch and Gonczy, 1998): (a) MT pushing through MT polymerization, (b) MT pulling through MT motor proteins or MT depolymerization, and (c) MTs acting as tracks on which the nucleus can travel using MT motor proteins. In budding yeast during G1 phase, MTs have been observed to push the nucleus (Shaw et al., 1997; Adames and Cooper, 2000). In many other cases, positioning of the nucleus and MTOC has been found to be dependent on MT-pulling forces that are often dynein dependent (Plamann et al., 1994; Xiang et al., 1994; Yeh et al., 1995; Gonczy et al., 1999; Koonce et al., 1999; Robinson et al., 1999).

The fission yeast *Schizosaccharomyces pombe* is a genetically tractable organism with a simple cytoskeleton and predictable cell shape and size. During interphase, the nucleus maintains its position at the geometrical center of the cell, even as the cell grows in an asymmetric manner from 7 to 14 μm in length (Mitchison and Nurse, 1985). Thus, nuclear positioning must be an active process that monitors the positions of the cell tips during cell growth. Nuclear positioning in *S. pombe* is dependent on MTs. For example, tubulin mutants display nuclear-positioning defects and defects in division site positioning, cell shape, and mitosis (Toda et al., 1983; Umesono et al., 1983; Radcliffe et al., 1998; Tran et al., 2000). In fission yeast, the positioning of the nucleus is important, since it appears to dictate the future plane of cell division (Chang and Nurse, 1996; Tran et al., 2000). In addition, the proper arrangement of MT ends at the cell tips also appears important for

✪The online version of this paper contains supplemental material.

Address correspondence to Phong Tran, Columbia University, 701 W. 168th St., Rm. 1404, New York, NY 10032. Tel.: (212) 305-3930. Fax: (212) 305-1468. E-mail: pt143@columbia.edu

[1]*Abbreviations used in this paper:* GFP, green fluorescent protein; iMTOC, interphase MTOC; MBL, methyl-2-benzimidazole-carbamate; MT, microtubule; MTOC, MT-organizing center; SPB, spindle pole body; TBZ, thiabendazole.

regulation of cell polarity in delineating regions of cell growth at the cell tips (Mata and Nurse, 1997; Hagan, 1998; Sawin and Nurse, 1998).

The interphase MT cytoskeleton has been studied primarily using immunofluorescence in fixed cells (Hagan, 1998). Multiple MT bundles extend along the long axis of the cell, forming a basket around the nucleus (Hagan and Hyams, 1988). EM of these interphase MTs has been difficult, but limited studies have revealed that some cytoplasmic MTs are arranged in small bundles (Hereward, 1974; Streiblova and Girbardt, 1980; Kanbe et al., 1989; Ding et al., 1997; Hagan, 1998). MT dynamics and organization and their role in nuclear positioning are poorly understood. The spindle pole body (SPB) organizes the spindle in the nucleus during mitosis, but its role in the interphase MT cytoskeleton is not yet clear (Hagan, 1998). The sites of MT nucleation and the polarity of MTs during interphase are not known. Time-lapse studies show that the interphase nucleus exhibits small rocking movements (Hagan et al., 1990; Hagan, 1998). It has been proposed that the SPB moves along an MT track (Hagan et al., 1990). However, in such a model the nucleus must somehow position itself on the MT track at the middle of the cell. It has been speculated that there may be gradients of putative signals that help to position the nucleus (Nurse, 1994; Chang and Nurse, 1996; Hagan, 1998).

Recent advances in imaging green fluorescent protein (GFP) fusion proteins in the living cells have allowed direct observation of MT behavior in fission yeast (Ding et al., 1998). Here, we report an analysis of the dynamic behavior of MTs and the nucleus. Our studies have led to a novel and unexpected model for MT organization and nuclear positioning that represents a significant change from previous models. We demonstrate that each linear MT structure is in fact a bundle of MTs organized in an antiparallel configuration, with the MT plus ends facing the two cell tips and minus ends near the nucleus. Instead of functioning as tracks, MTs may function in nuclear positioning by exerting pushing forces on the nucleus through MT polymerization. Thus, our studies establish a new mechanism for nuclear positioning and demonstrate how a cell may use dynamic MTs as intracellular rulers to define its middle.

Materials and Methods

Cell Strains and Preparations

Standard *S. pombe* genetics techniques and media were used as described (http://pingu.salk.edu/users/forsburg/plasmids.html#protocols and http://www.bio.uva.nl/pombe/handbook/). Five haploid strains were used in this study: PT.1 (*h⁻ ade6-M210 leu1-32 ura4-D18*, *GFP-cmd1*) (Moser et al., 1997); PT.47 (*h⁻ leu1-32 nmt-GFP-atb2*) (pDQ105) (Ding et al., 1998); PT.53 (*h⁻ leu1-32 nup107-GFP*); PT.65 (*h⁻ leu1-32 nup107-GFP nmt-GFP-atb2*); and PT.104 (*h⁻ leu1-32 sad1-GFP*) (pTN501) (Goshima et al., 1999). pDQ105 was a gift from Drs. D.-Q. Ding and Y. Hiraoka (Kansai Advanced Research Center, Communications Research Laboratory, Kobe, Japan). pTN501 was a gift from Drs. G. Goshima and M. Yanagida (Kyoto University, Kyoto, Japan).

We constructed the nup107-GFP strain as follows: a BLAST search at the Sanger Centre *S. pombe* server for proteins similar to murine NUP107p (Radu et al., 1994) and *S. cerevisiae* Nup84p (Siniossoglou et al., 1996) identified the *S. pombe* ORF SPBC582-11C, SPBC428.01C, encoding a 90-kD protein. Because of its similarity to murine NUP107, we named this gene *S. pombe nup107* and the corresponding protein nup107p. GFP tagging of the *S. pombe nup107* gene in its chromosomal location at the COOH terminus of *nup107* was done by a PCR-based approach as described by Bahler et al. (1998) using the pFA6a-GFP-kanMX6 plasmid (Wach et al., 1997) and the following oligonucleotides: forward primer, GGCAGACTGGTTGAATATGTTTCTTATTTAGGAAAGGCCGGAGAATGTAGCCTTTCAACCCCTAATGGGCTTTTTTCTTTAGGTCGACGGATCCCCGGG; and reverse primer, GTTTTTCAGCTTAGTTTTAAAATCAACGTATTAAGATAAACTGGTTATCAATGCGAAGATGATACCACATTTGCAGCATCATCGATGAATTCGAGCTCG. The resulting PCR product was transformed into the haploid strain (*h^90 ade6-210 leu1-32 ura4-D18*). G418-resistant transformant cells were screened by PCR for integration of the DNA fragment using the following primers: GACGAGGGGAAATTAATAGG (in the kanMX6 module) and GAACTTGCGCAATGGTCC (in the 3′ noncoding region of *nup107*). The localization of the nup107-GFP fusion protein analyzed in two independent positive clones revealed a perinuclear ring-like staining typical for nuclear pore labeling. This SpNup107-GFP fusion nucleoporin was functional, since it could rescue the lethal defect of a *nup107Δ* deletion mutant. The *nup107-GFP* strain was crossed with strain PT.3 (*h⁻ leu1-32*) to produce PT.53.

In preparation for microscopy, cells were grown in 4-ml shaking cultures at 25°C to midlog phase. Cells carrying pDQ105 (*nmt-GFP-atb2*) (Ding et al., 1998) were grown in EMM plus 5 μg ml^{-1} thiamine to repress the *nmt* promoter to a low level. 1 ml of cells was pelleted in a microfuge at 10,000 *g* for 15 s and then resuspended in 100 μl of medium. A 10-μl vol of the cells was then placed in a sealed agarose chamber. The chamber was constructed as follows: 2% wt/vol agarose (GIBCO BRL; UltraPure Agarose, Life Technologies) in YE5S was heated to 100°C; 50 μl of the melted agarose was placed on a clean glass slide (Micro Slides), and a second glass slide was immediately placed on top of the agarose droplet to flatten it into a pad; after 2 min, the top glass slide was removed, 1 μl of cells was placed on the agarose pad and covered with a clean glass coverslip (no. 1 1/2, 22 mm^2; Micro Slides); and the chamber was then sealed with valapa (1:1:1 vaseline/lanolin/paraffin). Chambers were made fresh for each experiment. Cells were viable and divided in chambers for several hours. Cells were imaged at room temperature, typically at 23–25°C. For MT inhibition studies, thiabendazole (TBZ) at a final concentration of 100 μg ml^{-1} (Sigma-Aldrich) or methyl-2-benzimidazole-carbamate (MBC) at a final concentration of 25 μg ml^{-1} (Aldrich Chemical Co.) was used. 100× stock solutions were made fresh in DMSO (Sigma-Aldrich) and added to both cell cultures and agarose in the chamber. For MT cold shock experiments, cells in medium were incubated in a 0°C water bath for 1 h.

Microscopy and Image Acquisition

Images were acquired digitally with either a real-time confocal microscope or a conventional wide-field epifluorescence microscope. For the real-time confocal microscope (Tran et al., 1999), we used the CSU-10 confocal scanning unit head (Yokogawa Electric Corp.) attached to the C-mount video port on top of a Leica DMRX upright microscope equipped with a Plan Fluotar 100×/1.3 NA oil immersion objective lens (Leica). An argon-krypton laser source with ~12 mW power at 488-nm excitation illuminated the scanning unit through an optical fiber (Omnichrome Corp.). Images were captured with a chilled Orca-1 CCD digital camera (C4742-95; Hamamatsu Photonics) controlled by MetaMorph Software (Universal Imaging Corp.) running on the Windows NT operating system with a 400 MHz Intel Pentium II.

For wide-field epifluorescence microscopy, we used a Nikon E800 upright microscope equipped with a Plan Apo 100×/1.4 NA DIC objective lens (Nikon) and GFP filter sets (Chroma Technology Corp.) illuminated with a 100 W mercury arc lamp. OpenLab Software (Improvision, Inc.) running on a 350 MHz Macintosh G3 controlled the excitation shutter (Vincent Associates), Z-motor (Conix Research), and Orca-1 CCD camera (Hamamatsu Photonics).

Time-lapse images were typically obtained at 2–5-s intervals in single optical section. Exposure times varied from 300 ms to 1 s. For fluorescent speckle microscopy (Waterman-Storer and Salmon, 1998; Waterman-Storer et al., 1998), cells expressing very low levels of GFP-tubulin were imaged with 1-s exposures. For some image sequences, Z-series optical sections through the cells at 0.5-μm spacing were taken spanning the ~4-μm cell diameter and then projected onto a single plane.

Data Analysis

Images were viewed with either the MetaMorph (Universal Imaging Corp.) or OpenLab (Improvision Inc.) imaging software. Rates of MT

growth and shrinkage were determined by measurement of changes in MT lengths from the time-lapsed sequences (Walker et al., 1988). MT length was determined by measuring individual MTs starting from the medial MTOC to the MT ends and converting pixels into microns using an image of a stage micrometer. Catastrophe and rescue frequencies were determined by observing the switching events over the total time of growth or shrinkage, respectively (Walker et al., 1988).

Displacements of the SPB or central MTOCs were measured by recording their X_N, Y_N coordinates through N successive frames. A center reference position (X_0, Y_0) was calculated as $(\Sigma X)/N$ and $(\Sigma Y)/N$, where N is the total number of position points. Displacement from this center reference position was then calculated as $D_N = \sqrt{([X_N - X_0]^2 + [Y_N - Y_0]^2)}$.

Lengths and displacements were plotted against time, and rates were determined by linear regression analysis using KaleidaGraph (Synergy Software). Only directed movements that remained linear for at least four consecutive time points were used to determine a rate. Two-tailed t tests were performed on our data sets using the Data Analysis package included in Microsoft Excel. KaleidaGraph was used to plot data sets. Canvas (Deneba Software) was used for figure presentation.

Intensity scans in Fig. 1 were done with the shareware NIH Image (http://rsb.info.nih.gov/nih-image/download.html). MT bundles in Fig. 1, A and B, were imaged with the real-time confocal microscope, thereby minimizing out-of-focus fluorescence. Digital images had an 8-bit dynamic range or 255 grey levels (0 = black, 255 = white). Outside the cell, the background had an average intensity of 65. The MT flanking the central higher fluorescent region had an average intensity of 130. The central higher fluorescent region had an average intensity between 170 and 190. Correcting for background contribution, the medial higher fluorescence region had approximately two times greater intensity than the flanking MT regions.

To quantify the difference between high and low GFP-tubulin expression levels (see Table I), area intensity scans were performed on individual MTs. The wide-field epifluorescence microscope was used to image bright cells at 300-ms exposure time and dim cells at 1-s exposure time. A rectangular region was boxed around the area representing the fluorescent MT, and its average intensity was measured. The high GFP expression level MTs were qualitatively very bright with no noticeable speckles and had an average measured area intensity of 135. Low GFP expression level MTs were dimmer by comparison with noticeable speckles and had an average measured area intensity of 56. The background had an average measured area intensity of 15. Correcting for background contribution and for exposure times, low GFP expression cells exhibited approximately ninefold less GFP-tubulin in their MTs than high GFP expression cells.

To compare the growth rates of the two ends of each MT bundle, we calculated the difference between the two tips of each MT bundle as an average maximal ratio. First, the average growth rates for the two sides of each MT bundle were obtained. Then, the ratio of the higher growth rates over the lower growth rates (maximal ratio) of each pair of MTs of each bundle was calculated and averaged for all MT bundles to obtain the average maximal ratio.

Computer Model for Nuclear Positioning

An iterative numerical analysis approach programmed in C++ was used to model the effects of MTs on nuclear localization. The following parameters, which match those observed in living cells, were used: MT growth rate = 2 μm min^{-1}; MT shrinkage rate after catastrophe = 9 μm min^{-1}; and cell length = 14 μm. A random number generator-based stochastic algorithm modeled MT tips as touching the cell surface for an average of 1.5 min. Stiffness of MTs was defined as proportional to the inverse of the square of MT length, mimicking the length-dependent critical buckling force. In the algorithm, MTs were modeled as being attached to the left or right of a single point representing the nuclear center. Nuclear displacement was determined by an algorithm that monitored whether the force on the nucleus generated by MT growth during a 1-s iteration was leftward (negative) or rightward (positive). The net force on the nucleus was set equal to the sum of all of the forces from all of the MTs (that is, MT displacement × MT stiffness). Nuclear position for each iteration was incremented leftward or rightward based on the sign of the net force acting on the nucleus. Maximum nuclear excursion during a 1-s iteration was ~0.03 μm (~0.2% of the cell length). MT variables and nuclear positions were calculated at 1-s intervals and sampled at appropriate times. Data were collected for analysis of nuclear displacement and distribution and written to Excel-readable files. The source codes of our program can be downloaded at http://cumicro2.cpmc.columbia.edu/Changlab/index.html.

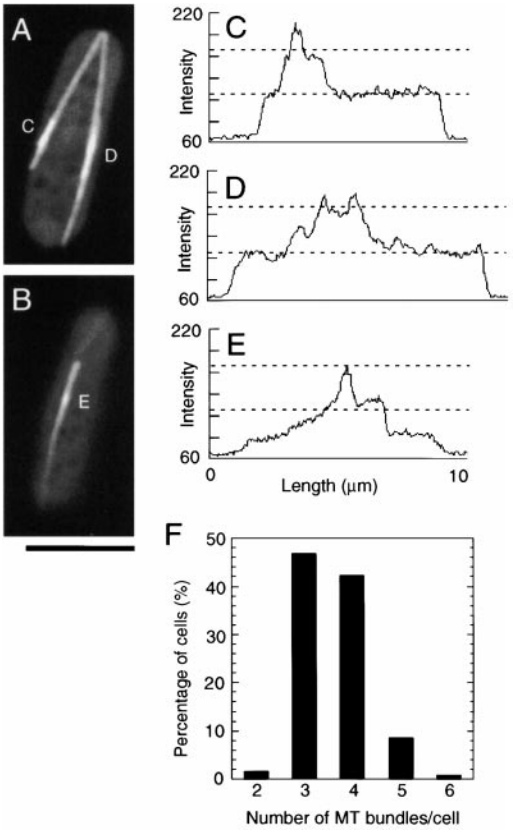

Figure 1. Organization of interphase MTs in multiple bundles with a medial overlap region. Wild-type cells expressing GFP-tubulin (PT.47) were imaged for GFP fluorescence using a confocal microscope. (A and B) Optical sections through a cell with three MT bundles. Each MT bundle contained a region of higher fluorescence intensity located near the cell center. (C–E) Intensity line scans along the length of each MT bundle labeled in A and B (see Materials and Methods). (F) Plot of the number of MT bundles per cell (n = 128 cells). Video available at http://www.jcb.org/cgi/content/full/153/2/397/DC1. Bar, 5 μm.

Online Supplemental Material

Supplemental videos are presented online at http://www.jcb.org/cgi/content/full/153/2/397/DC1. The seven videos depict a three-dimensional reconstruction of the MT cytoskeleton, dynamics of the nuclear envelope and sad1p, and dynamic effects of MTs on the nuclear envelope.

Results

Organization of Interphase MTs in Antiparallel MT Bundles: Plus Ends Are Oriented toward the Cell Tips

To visualize the structural arrangement and the dynamics of the MT cytoskeleton, we used a combination of wide-field fluorescent microscopy and real-time confocal microscopy to image living fission yeast expressing a fusion protein of GFP to the α-tubulin protein atb2 (Ding et al., 1998). This GFP-tubulin fusion has been used previously for the visualization of the MT cytoskeleton in fission yeast (Ding et al., 1998; Chang, 1999; Tran et al., 1999, 2000; Yamamoto et al., 1999; Bezanilla et al., 2000; Paluh et al., 2000). Expression of this GFP-tubulin did not affect cell growth rate, cell shape, cell length, or MT organization

Table I. Measured Parameters of S. pombe Interphase MT Dynamics

		MTs, cells
		n
MT growth rate V_g		
High GFP-tubulin expression level	1.86 ± 0.54 μm min^{-1}*	67, 26
Low GFP-tubulin expression level	1.90 ± 0.33 μm min^{-1}*	7, 4
Before tip contact	2.08 ± 0.53 μm min^{-1}‡	17, 10
After tip contact	1.30 ± 0.44 μm min^{-1}‡	17, 10
Average maximum ratio	1.35 ± 0.33	31, 23
MT shrinkage rate V_s		
High GFP-tubulin expression level	8.99 ± 2.82 μm min^{-1}§	64, 26
Low GFP-tubulin expression level	9.50 ± 3.85 μm min^{-1}§	7, 4
MT catastrophe frequency f_{cat}	0.31 min^{-1}‖	49, 19
MT rescue frequency f_{res}	0 min^{-1}¶	49, 19
Duration of MT cell tip contact before catastrophe	1.50 ± 0.59 min	179, 33

Rates were determined by linear regression analysis of each MT analyzed over 5–20 displacements measured 2–5 s apart. Data are given as mean ± SD of the rates measured for each MT, with *n* = number of MTs and cells measured.
*T test showed no significant differences ($P \geq 0.05$) between values.
‡T test showed no significant differences ($P > 0.05$) between values.
§T test showed no significant differences ($P \geq 0.05$) between values.
‖49 events/158 min total growth time.
¶0 events/30 min total shrinkage time.

compared with MT distribution seen by immunofluorescence of fixed cells (Hagan, 1998).

Here, we characterized the MT cytoskeleton of interphase cells 9–14 μm in length at 23–25°C. GFP-tubulin revealed multiple discrete bundles of MTs that run mostly parallel to the long axis of the cell (Fig. 1, A and B). Examination of cells in all focal planes revealed that most cells have three to four MT bundles (Fig. 1 F and video 1 available at http://www.jcb.org/cgi/content/full/153/2/397/DC1; Yamamoto et al., 1999). Each MT bundle had an area of higher GFP-tubulin fluorescence intensity near the center region of the cell. The length of this brighter region was variable (0.84 ± 0.29 μm; *n* = 43 MT bundles in 13 cells). Fig. 1, A and B, show two confocal optical sections of an interphase cell that contains a total of three MT bundles. Intensity scans along the length of each MT bundle yielded peak intensities at these medial regions two- to threefold higher than those intensities of the flanking MTs (Fig. 1, C–E), suggesting that there are two to three times more MTs in these central regions than in the rest of the bundle. The dynamic behavior of each MT bundle, described below, suggested that there was one MT in the lower intensity regions toward the tip and two to three MTs at the central high intensity region.

The interphase MTs were highly dynamic. Cells were imaged at 2–5-s intervals in single focal planes to obtain high temporal resolution; however, similar results on MT dynamics were also obtained in three-dimensional sections (our unpublished observations). Table I summarizes the measured parameters of MT dynamics in the fission yeast. Growth rates of ~2 μm min^{-1} and shrinkage rates of ~9 μm min^{-1} were comparable to rates for MT plus ends measured in vitro with purified tubulin (Horio and Hotani, 1986; Walker et al., 1988; Gildersleeve et al., 1992) or in vivo in other eukaryotes (Verde et al., 1992; Carminati and Stearns, 1997; Shaw et al., 1997; Adames and Cooper, 2000; Maddox et al., 2000). To test whether expression of GFP-tubulin may alter MT dynamics, we analyzed MT dynamics in cells expressing high and low levels of GFP-tubulin fluorescence. At low levels, speckles of GFP fluorescence were seen (see Fig. 3 A), suggesting that only ~1–5% of the total MT polymer was composed of GFP-tubulin (Waterman-Storer and Salmon, 1998; Waterman-Storer et al., 1998). No significant differences in MT dynamics were found at these different expression levels (Table I), suggesting that our use of GFP-tubulin at these expression levels did not perturb MT dynamics.

Although each half of an MT bundle behaved independently, the two halves exhibited similar behaviors with similar dynamics (Fig. 2 B and Table I). Both ends of an MT bundle grew at an average rate of 1.86 ± 0.54 μm min^{-1} from the medial-bundled region toward the cell tip (Table I). When growing MTs contacted the tip of the cell, they continued to grow, sometimes producing a bowed or buckled MT. The rate of MT polymerization was significantly slower in some MTs when the MT abutted the cell tip (an average decreased growth rate to 1.30 ± 0.44 μm min^{-1} after touching the cell tip, an ~38% decrease from 2.08 ± 0.53 μm min^{-1} growth rate before touching the cell tip) (Table I), consistent with a stall force slowing down MT growth rates (Dogterom and Yurke, 1997). At the cell tip, the MT remained in contact with the tip region for 1.50 ± 0.59 min (Table I) before exhibiting catastrophe and shrinking back to the medial MT-bundled region at the nucleus. MTs did not depolymerize beyond this medial region. No rescue events were seen until MTs shrank back to the medial-bundled region (Fig. 2 B). After shrinkage to the medial region, MTs began to regrow from this site immediately. Depending on length of the cell and MT, each growth and shrinkage cycle lasted 4–6 min.

To understand the organization of MTs, one important question is the polarity of the MTs. We considered two models: (a) the MTs may be organized in a parallel configuration so that the polarity of the ends of the bundle would be different, and (b) MTs may be organized in an antiparallel configuration so that the polarity of the ends of each bundle would be the same. To examine the polarity of the MTs at the ends of the bundle, we compared their growth rates. The inherent asymmetry in the polarity of the MT confers differential dynamics at the ends of an

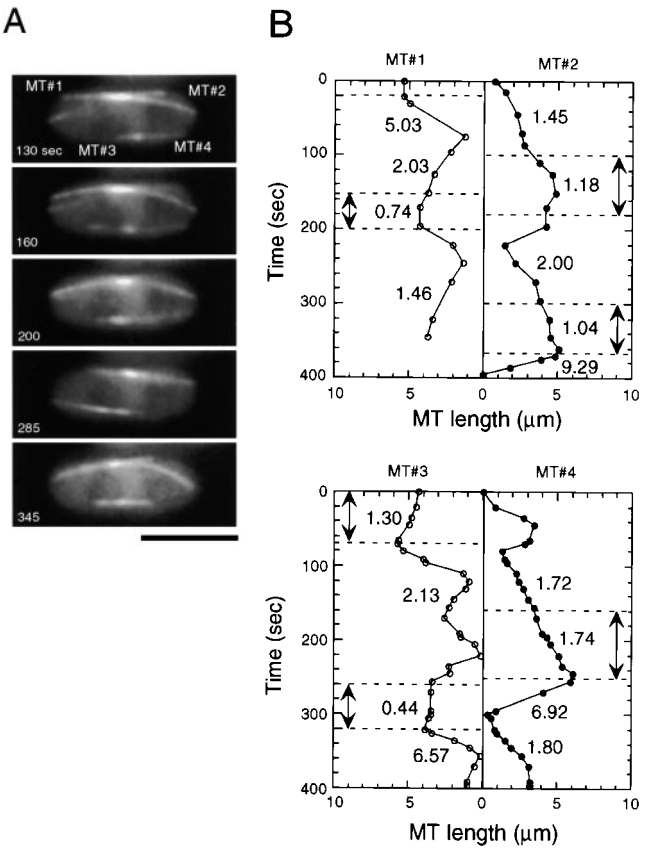

Figure 2. Dynamics of MTs show that both ends of an MT bundle behave in a similar manner. Cells expressing GFP-tubulin (PT.47) were imaged for GFP fluorescence. (A) Time-lapse sequences of two MT bundles in the same optical section. A third MT bundle that goes in and out of the present focal plane was not included in the analysis. (B) Plots of changes in MT lengths over time in this cell. MT#1, 2, 3, and 4 denote plots of each MT labeled in A. Position zero indicates the initial position of the medial region of higher fluorescence intensity. The double arrows indicate the time period each MT end touched the cell tip. Numbers show the rate of MT growth or shrinkage in each period in μm min^{-1}. Each tip of an MT bundle behaved independently of the other tip but exhibited similar dynamic parameters. Bar, 5 μm.

MT (Desai and Mitchison, 1997); for instance, for purified MTs in vitro minus ends can exhibit threefold lower growth rates than plus ends (Horio and Hotani, 1986; Walker et al., 1988). We found that the average maximum ratio of growth rates (see Materials and Methods) between the two ends of a bundle was 1.35 ± 0.33 (n = 31 MT bundles), with the lowest ratio being 1.00 and the highest ratio being 2.14. Given the variability in MT dynamics in vivo and assuming that minus and plus ends in *S. pombe* have comparable differences, this analysis suggested that the two ends of each MT bundle have the same polarity. Thus, the bundles may be arranged in an antiparallel configuration with the medial high intensity region as a region of overlap.

To determine further the polarity and sites of tubulin polymerization and depolymerization, we used fluorescent speckle microscopy to observe fiduciary marks on the MT lattice (Waterman-Storer and Salmon, 1998; Waterman-Storer et al., 1998). MT fluorescent speckles arise from random incorporation of a small amount of labeled tubulin into the MT lattice (Waterman-Storer and Salmon, 1998; Waterman-Storer et al., 1998) and provide fiduciary marks in the MT lattice. Since GFP-tubulin was expressed from a plasmid with variable copy number, it was possible to identify cells that expressed very low levels of GFP-tubulin. Imaging of these cells revealed speckles of GFP fluorescence on the MT lattice. Analysis of fluorescent MT speckles showed that the large bulk of tubulin polymerization and depolymerization occurred at the MT ends facing the cell tips (Fig. 3; n = 15 cells). Little or no movement of speckles occurred at the medial region between the MT lattice and the medial-bundled region. The dynamics of *S. pombe* MTs at cell tips were similar to the plus end dynamics of MTs in other organisms, suggesting that MTs at the cell tips of *S. pombe* are plus ends and that the minus ends are contained within the medial-bundled region.

This speckle analysis also showed that MT bundles exhibit lateral movement. When MTs continued to grow while abutting the cell tip, the entire MT bundle, including the central bundled region and the MT on the other side of the cell, moved away from that cell tip (Fig. 3 and see Fig. 8). This behavior suggested that the MT bundle may be pushed by MT polymerization at the cell tip.

MT Bundles Are Organized from Multiple Organizing Centers

Our analysis of MT dynamics showed that they grew from and shrank to multiple sites near the nucleus. To define these regions further, cells were treated with 25 μg ml^{-1} MBC, an MT-depolymerizing drug, for 5 min. MBC-treated cells exhibited multiple GFP-tubulin dots or stubs near or on the nucleus (Fig. 4 A). In cells not expressing GFP-tubulin, similar tubulin spots were seen by immunofluorescence of MBC-treated or cold-treated cells (our unpublished observations) (Mata and Nurse, 1997; Chen et al., 1999). Fig. 4 B shows that interphase cells contain two to four stable MT dots. The number of stable MT dots per cell was similar to but slightly less than the number of MT bundles per cell (compare Fig. 1 F with Fig. 4 B), suggesting that each MT bundle contained one medially located stable region. The difference in the number of dots in MBC-treated cells compared with the number of MT bundles may be caused by the ability of MBC to depolymerize some of the stable regions, by clustering of some of these spots upon MBC treatment, or by the possibility that some MTs do not have a stable region.

Next, we tested the relationship between these stable MT dots and the normal MT bundles by observing the regrowth of the MT cytoskeleton from these stable regions after depolymerization. MTs were depolymerized to medial spots or short fragments by cold shock. Cells were then shifted to room temperature and immediately imaged. The elapsed time between temperature shift and the first obtained image was ~30 s, during which time the MTs had already begun to repolymerize. Each MT dot or stub, which was positioned close to the nucleus (time 0.5 min; Fig. 4 C), rapidly repolymerized into a long-bundled MT very similar to a normal interphase MT. MTs elongated from two ends of each of the stable dots with similar rates. The subsequent medial-bundled region overlapped with

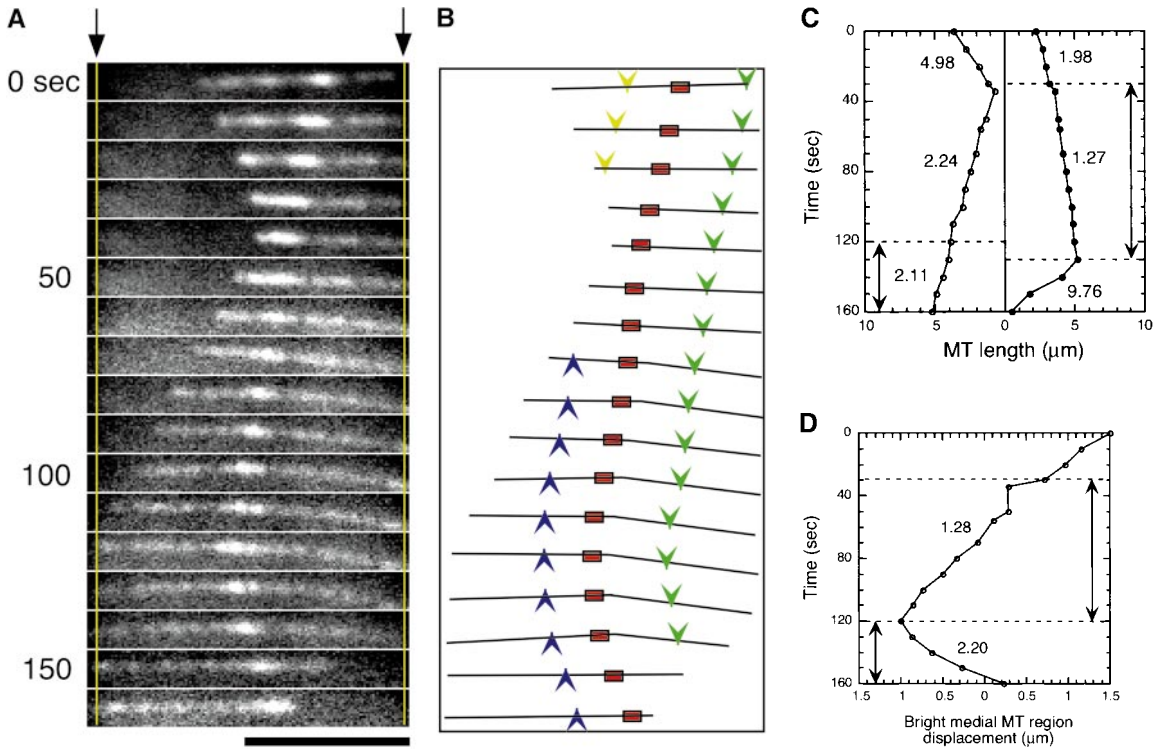

Figure 3. Fluorescent speckle microscopy analysis of an MT bundle. PT.47 cells expressing low levels of GFP-tubulin were imaged for GFP fluorescence (see Materials and Methods). (A) Time-lapse sequences of a single MT bundle with GFP-tubulin speckles. Arrows and lines mark the tips of the cell. (B) Trace of the images in A. Color arrows label regions of speckles, and the red rectangle denotes the medial-bundled MT region. (C) Plot of changes in MT lengths over time. Position zero indicates the position of the region of the medial MT-bundled region. (D) Plot of the position of the higher fluorescence intensity region over time. Position zero indicates the mean position. The double arrow lines indicate the period over which each MT end contacted with the cell tip. Numbers show the rate of MT growth or shrinkage in each period in μm min^{-1}. The MT exhibited growth and shrinkage at the distal tips of the MT bundle with little change at the medial portion of the bundle. The whole MT lattice along with the medial MT-bundled region moved away from the cell tip when the MT touched the cell tip.

but was generally larger than the initial stable MT dot. No de novo nucleation of MTs in the cell cytoplasm was observed. Short MT bundles had no preferred orientation within the cell, but as they grew they contacted the side of the cylindrical cell and were oriented into the longitudinal orientation through elongation. MT ends did not catastrophe when they touched the sides of the cell, only when they contacted the cell tips. These findings demonstrate that the interphase MT cytoskeleton is organized from multiple MTOCs on or near the nucleus that are stable to depolymerization.

MTs Are Required for Nuclear Positioning and Nuclear Movements

Previous work suggested that the positioning of the nucleus is an MT-dependent process, but these analyses were complicated by abnormal mitoses and "cut" events that can cause mislocalization of nuclear components (Walker, 1982; Toda et el., 1983; Umesono et al., 1983; Beinhauer et al., 1997; Radcliffe et al., 1998). We reexamined the effects of MT disruption on nuclear positioning specifically during interphase using MT-depolymerizing agents. To observe the nucleus, we used a functional GFP fusion to a putative nuclear pore protein, Nup107 (see Materials and Methods). Cells expressing this fusion were treated with MBC for 2 h at 25°C. To avoid mitotic effects, we used time-lapse microscopy to assay cells that stayed in interphase for the period. 100% (n = 20) of nuclei in untreated cells were located at the geometric center of the cell (±10% of the cell length), whereas only 41% (n = 37) of nuclei in MBC-treated cells were located in this medial region. These data were consistent with previous findings (Walker, 1982; Toda et el., 1983; Umesono et al., 1983; Beinhauer et al., 1997; Radcliffe et al., 1998; Tran et al., 2000) and indicated that MTs are required for efficient accurate positioning of the nucleus during interphase.

To examine the effects of MTs on the nucleus more closely, we measured SPB dynamics. The SPB is associated with the nucleus and one of the MT bundles during interphase (Ding et al., 1997; Hagan and Yanagida, 1995). We used GFP-cmd1p as a marker for the SPB (Moser et al., 1997). Time-lapse microscopy revealed that the SPB oscillated largely in a direction parallel to the long axis of the cell (Fig. 5 A), with an average rate of 1.30 ± 0.36 μm min^{-1} and a maximum excursion length of 2.62 ± 0.57 μm (Table II). To test if this movement was MT dependent, cells were treated for 5 min with 100 μg ml^{-1} TBZ, an MT-depolymerizing drug. In TBZ-treated cells, SPB movement was greatly diminished with no noticeable directed movement and its maximum excursion length decreased to 0.67 ± 0.15 μm (Fig. 5 B and Table II). These effects were seen in

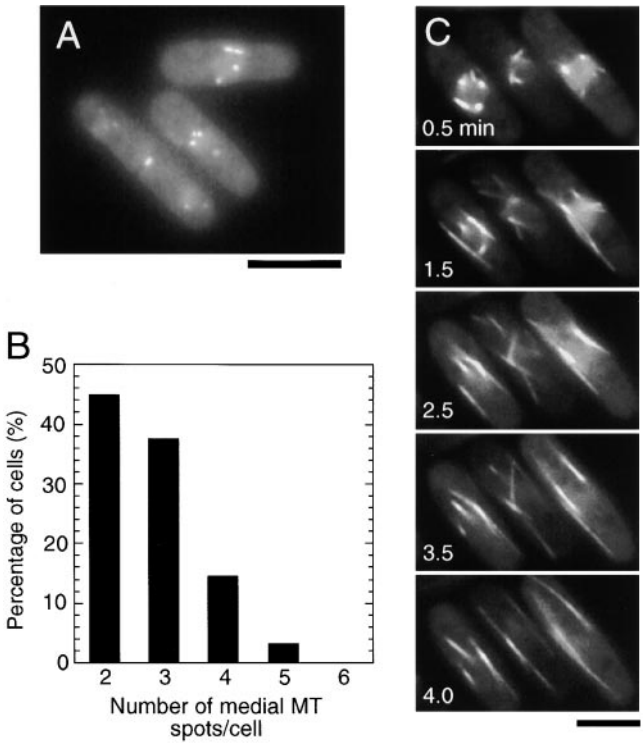

Figure 4. MTs are organized from multiple medial stable dots near the nucleus. (A) Cells expressing GFP-tubulin (PT.47) were treated with 25 μg ml^{-1} MBC for 5 min at 25°C. Interphase cells exhibited discrete dots or short fragments of GFP-tubulin staining. The bottom left cell is in cytokinesis/septation, and the GFP-tubulin labeled the postanaphase MTOC at the septum and faint GFP-tubulin dots near the two nuclei located near the cell tips. (B) The number of MT dots per interphase cell after MBC treatment (n = 96 cells). (C) Time-lapse sequences of MT repolymerization after depolymerization from cold treatment. PT.47 (GFP-tubulin) cells were incubated on ice for 1 h and then placed on a slide and imaged at room temperature (23–25°C). Time denotes time after temperature shift. MTs rapidly repolymerized from both ends of each of the medial MT fragments. Bar, 5 μm.

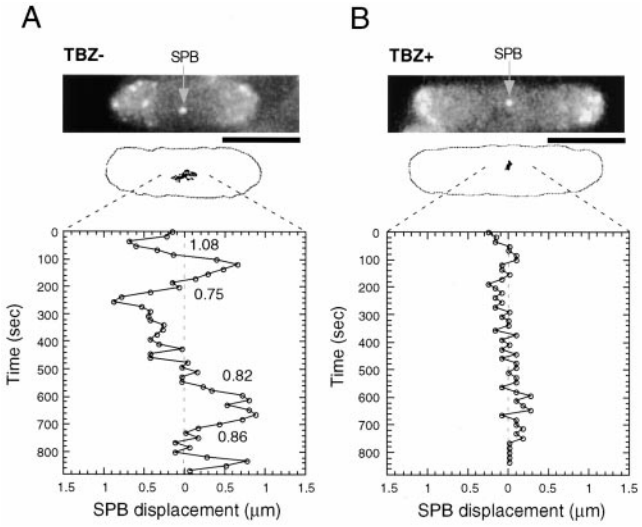

Figure 5. MT-dependent oscillation of the SPB. Cells expressing cmd1-GFP (PT.1) exhibited labeling of a medial SPB (arrow) and non-SPB patches (possibly actin patches) at the cell tips (Moser et al., 1997). The SPB was clearly distinguished from the patches by its position and dynamics. SPB dynamics in an untreated wild-type cell (A) or in a cell treated with 100 μg ml^{-1} TBZ for 5 min (B). The top shows an image of the cell with the medial fluorescent SPB; the middle shows tracings of the path of the SPB in a time-lapse sequence of ~14 min; and the bottom shows plots of SPB displacement from a mean position over time. Bars, 5 μm.

all the TBZ$^+$ cells examined (n = 21). Thus, the SPB oscillates in an MT-dependent manner.

We used GFP-nup107 to examine the dynamics of the nuclear envelope. nup107-GFP labeled the nuclear envelope in a patchy manner. Time-lapse microscopy revealed that the nuclear membrane exhibited frequent and transient deformations, giving the nucleus a nonspherical shape (Fig. 6 A and video 2 available at http://www.jcb.org/cgi/content/full/153/2/397/DC1). In cells treated for 5 min with 100 μg ml^{-1} TBZ, the nuclear envelope did not exhibit these deformations and maintained a spherical shape (Fig. 6 B and video 3 available at http://www.jcb.org/cgi/content/full/153/2/397/DC1). These effects were seen in all the cells examined (30 TBZ$^-$ cells and 15 TBZ$^+$ cells).

To visualize both the SPB and the nuclear envelope, we imaged a strain that mildly overexpresses a sad1-GFP fusion protein (Goshima et al., 1999). sad1p is a transmembrane protein component of the SPB (Hagan and Yanagida, 1995), and overexpression of sad1-GFP not only labeled the SPB and nuclear envelope but also labeled less intense discrete spots on the nuclear membrane (Goshima et al., 1999), which have not been visualized by immunofluorescence (Hagan and Yanagida, 1995). Approximately 85% of cells (n = 38) with bright sad1-GFP fluorescence contained one to three of these discrete sad1-GFP dots in addition to the major SPB dot. Time-lapse microscopy clearly showed deformations at the nuclear envelope at multiple points in all cells (n = 33 cells) (Fig. 6 C and video 4 available at http://www.jcb.org/cgi/content/full/153/2/397/DC1). In all cases, the SPB was associated with major deformations in the nuclear envelope (n =

Table II. Comparison of SPB Movement, MT Growth Rate at the Cell Tip, and Nuclear Envelope Movement

	Rate	Maximum excursion length	MTs, cells
	μm min^{-1}	μm	n
SPB movement (−TBZ)	1.30 ± 0.36*	2.62 ± 0.57	NA, 40
SPB movement (+TBZ)	NA‡	0.63 ± 0.15	NA, 21
MT gowth at cell tip	1.46 ± 0.49*		35, 26
Movement of MT bundled region and nuclear envelope	1.36 ± 0.49*		35, 26

Data are given as mean ± SD of the rates measured for each SPB or MT, with n = number of MTs and cells measured.
*T test showed no significant differences ($P \geq 0.05$) among values.
‡No rate was determined since no linear movements over 1 min were observed.

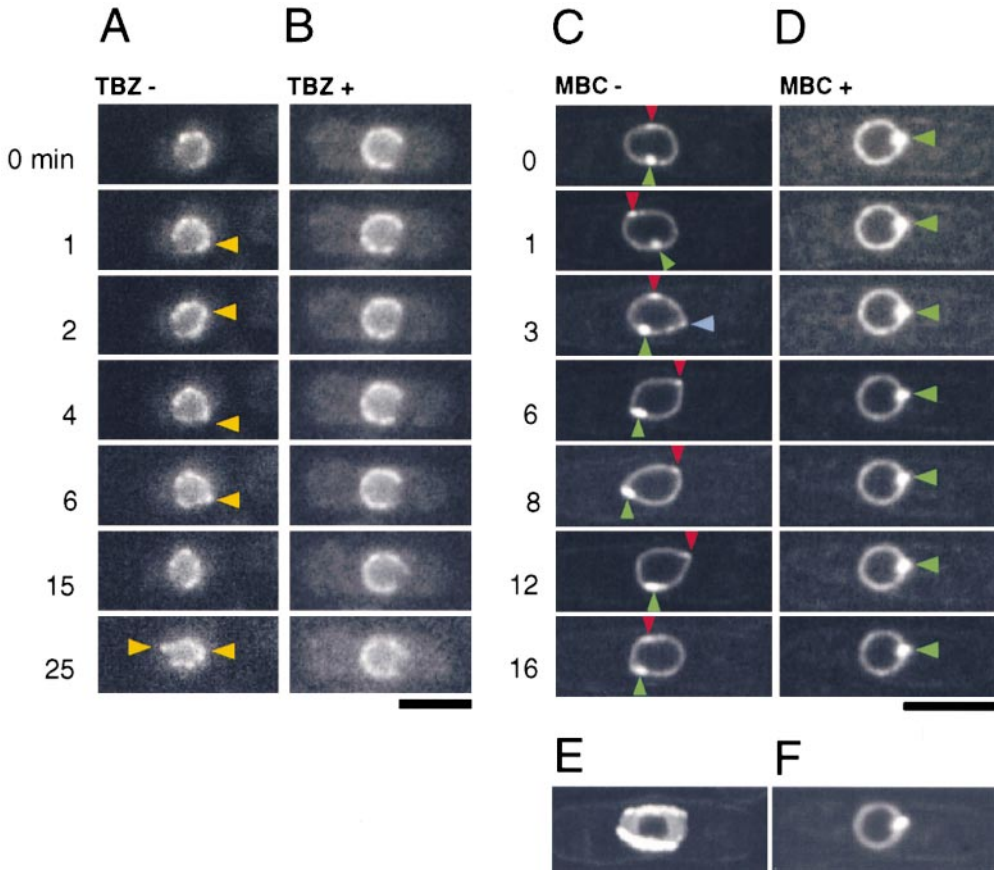

Figure 6. MT-dependent movement of the nuclear membrane. PT.53 cells expressing the nuclear pore marker nup107-GFP and PT.104 cells expressing sad1-GFP were either treated for 5 min with 100 μg ml^{-1} TBZ (B), 25 μg ml^{-1} MBC (D), or not treated (A and C) and then imaged for GFP fluorescence in time-lapse using wide-field (A and B) or confocal (C and D) microscopy. (A) The nuclear envelope exhibited frequent deformations or displacements at multiple locations (arrows). (B) Cells treated with TBZ, the nuclear envelope appeared rounder, without deformities. (C) PT.104 cells exhibited a major dot (SPB, green arrow) and often one to three other minor dots (red and blue arrows). Both the SPB and minor dots were associated with nuclear envelope deformations (for example, red arrow at 6 min and green arrow at 8 min). Time-lapse sequence showed that the dot labeled by the blue arrow was distinct from the other two dots. (D) PT.104 cells treated for 5 min with MBC exhibited a rounder nucleus without deformities. Videos available at http://www.jcb.org/cgi/content/full/153/2/397/DC1. (E) Superimposed image of multiple time-lapse images in C, which shows the sum excursions of the SPB and a minor sad-GFP dot. (F) Superimposed image of multiple time-lapse images in D. Bars, 5 μm.

33 cells). However, it was apparent that many deformation events were spatially independent of the SPB. In cells where a major sad1-GFP dot (the SPB) and a minor sad1-GFP dot (n = 10 cells) were imaged in the same optical section, the minor sad1-GFP dot was also associated with nuclear membrane deformations. The SPB and the minor sad1-GPP dots moved in a similar oscillatory manner, generally in flattened arcs along the cell longitudinal axis (Fig. 6 E) but moved independently, suggesting that the whole nuclear envelope was not merely rotating. Maximal excursion lengths of the sad1-GFP–labeled SPB, the cmd1-GFP–labeled SPB, and minor sad1-GFP dots were similar (Fig. 5 and Fig. 6 E). Some deformation events were not associated with any sad1-GFP dot, although we could not rule out that sad1-GFP dots were out of the plane of focus. In cells treated for 5 min with 25 μg ml^{-1} MBC, no deformations were observed, and the SPB was stationary (Fig. 6 D and video 5 available at http://www.jcb.org/cgi/content/full/153/2/397/DC1) (n = 15 cells). Thus, both these sad1-GFP and the nup107-GFP studies show that the nucleus constantly experiences small movements or deformations through MT-dependent forces acting on the SPB and other sites on the nuclear envelope.

MT Bundles Push the Nucleus

To visualize how MTs may move the nuclear envelope, we next imaged cells expressing both nup107-GFP and GFP-tubulin. MTs and the nuclear envelope exhibited dynamics as observed above. Videos 6, 7, and 8 (available at http://www.jcb.org/cgi/content/full/153/2/397/DC1) show the dynamic behavior of MTs and nuclear pushing events. Fig. 7 presents the analysis of a representative cell in which two MT bundles in the focal plane were closely associated with the nuclear membrane at the central-bundled MT region (Fig. 7 A, color arrows). Positions of the MT tip, central-bundled region, and nuclear envelope were analyzed. In the top MT bundle, the central-bundled region moved to the right when the left MT, MT#1, touched the left cell tip and continued to grow for 1.5 min (Fig. 7 B). MT length increased steadily at a velocity of 1.03 μm min^{-1}, whereas the central-bundled region and the nuclear envelope moved with a similar velocity of 0.98 μm min^{-1}, leading to ~1.5 μm of MT polymerization giving 1.4 μm displacement of the nuclear envelope. These movements suggested that the MT pushed the nucleus at rate of MT polymerization. Progressive buckling of the MT (MT#1 in Fig. 7 A) further demonstrated that the MT exerted a pushing force and that MT must be attached to the nucleus, which exerted forces resisting movement. After 1.5 min at the cell tip, the MT (MT#1 in Fig. 7, A and B) started to shrink. The MT stopped buckling and the MT central-bundled region and nuclear envelope immediately began to move back to the right in a less directed fashion. The nuclear membrane reformed into a more spherical shape,

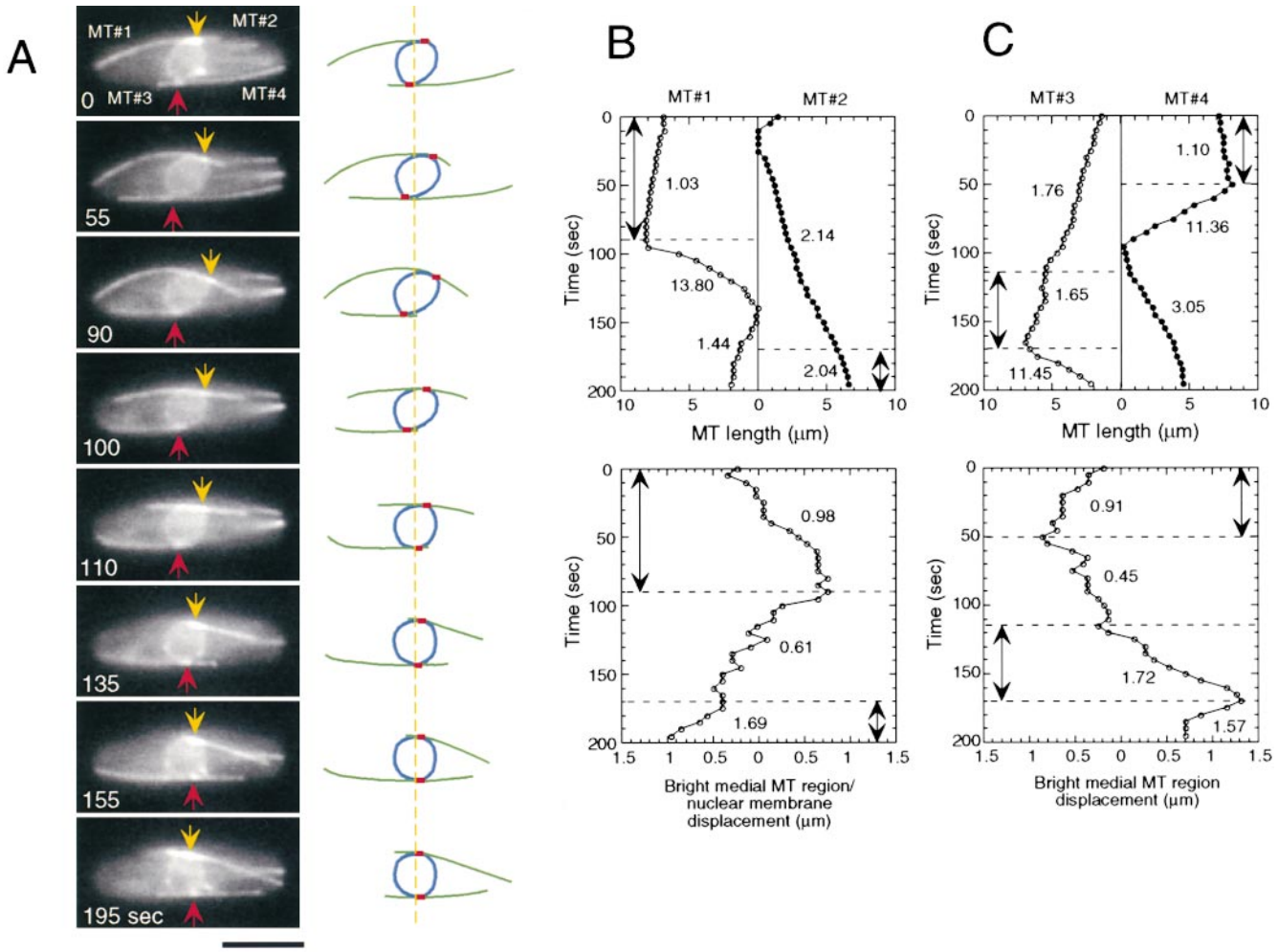

Figure 7. MT bundles give transient pushes on the nuclear membrane. Cells expressing both GFP-tubulin and nup107-GFP (PT.65) were imaged in a single optical plane in time-lapse. (A) Representative images are shown, with arrows pointing to regions of bundled MTs that appear to be attached to the nucleus. Tracings of these images are shown on the right, with the MTs (green), nuclear envelope (blue), and regions of bundled MTs (red). Note that the nuclear envelope and the bundled MT region (red) move away from the cell tip only during the period when the MT contacts the cell tip. (B and C) Plots of MT dynamics (top) and displacement of these medial MT-bundled regions (bottom) in the cell shown in A. The double arrow lines indicate the period during which each MT end maintained contact with the cell tip and which tip it contacted; arrow on the left denotes that the left MT contacted the left cell tip. Numbers show the rates of growth or shrinkage during each period in μm min^{-1}. Note the rates and periods of MT polymerization at the tip correspond to movement of the central-bundled region and of the nuclear envelope. Videos available at http://www.jcb.org/cgi/content/full/153/2/397/DC1. Bar, 5 μm.

possibly from elastic recoil in the nuclear envelope or from other forces from opposite MT bundles not present in this focal plane. Similar pushing events were found at the right half of the same MT bundle (MT#2 in Fig. 7 A) that pushed the nuclear envelope to the left.

This example demonstrates that this MT bundle is attached to the nucleus and pushes it as the MT polymerizes at the cell tip. This behavior was not consistent with pulling or tracking models. Pulling forces would cause the nucleus to move toward the cell tip when the MT reached the cell tip and would produce straight MTs under tension, not buckled ones under compression. These results were also not consistent with a tracking model: the one-to-one correlation between the rates of MT elongation while touching the cell tip, the movement of the medial MT-bundled region, and the displacement of the nuclear envelope (Table II) suggested that the nucleus did not move relative to the MT lattice.

Analysis of sad1-GFP nuclei suggested that multiple MT bundles may be attached to the nucleus (Fig. 6 C). In Fig. 7, a second MT bundle in the lower part of the same cell (MT#3 and 4) and a medial-bundled region moved in a similar manner dependent on pushing events, but the deformation of the nuclear envelope was less clear. In confocal analysis of many other cells (n = 84), pronounced nuclear deformations were detected generally (but not always) from only one site, in contrast to the sad1-GFP fusion, which showed multiple sites of deformation. This difference may be due to: (a) difficulties in visualizing the deformations because of the patchy nature of nuclear pore marker and overlapping fluorescence from the MTs, or (b) possible differences caused by the expression of the fusion markers.

To test further the MT pushing mechanism, we used fluorescent speckle analysis to correlate the movement of the

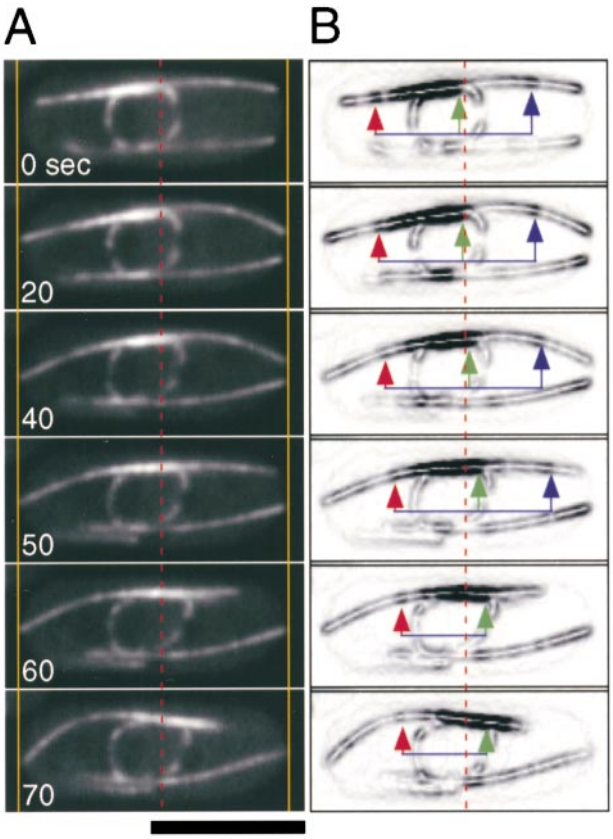

Figure 8. Fluorescent speckle microscopy shows that the nuclear envelope moves with the MT lattice. Cells expressing both GFP-tubulin and nup107-GFP (PT.65) were imaged in a single optical plane in a 70-s time-lapse sequence. (A) GFP fluorescence time-lapse images. Time is shown in seconds. Yellow lines mark the cell tips, and the dotted red line indicates the initial point where the MT and the nuclear membrane touch. (B) "Edge-enhanced" images of images shown in A. This image enhancement highlights MT speckles. Red arrows point to a speckle on the left MT, green arrows point to a site on the nuclear envelope that appears attached to the MT, and blue arrows point to a speckle on the right MT. The distances between the colored arrows remained equidistant as the MT bundle moved and distorted the nuclear membrane. Bar, 5 μm.

MT lattice with the movement of the nuclear envelope (n = 15 cells). Time-lapse images in Fig. 8 show displacement of the nuclear envelope by a growing MT. Like in Fig. 3, the pattern and movement of MT speckles (see red arrow) indicated that an MT (top left) elongated by addition of subunits at its distal end, and as the MT end contacted the left cell tip, the MT lattice was pushed to the right. The movement of the MT lattice to the right corresponded to a rightward movement of the central-bundled MT region and a rightward stretch of the nuclear membrane (green arrow) by the same distance. Thus, this fluorescent speckle microscopy analysis showed that the nucleus moved with the MT lattice and did not move relative to the MT lattice.

To test how general this pushing mechanism is, we analyzed time-lapse sequences of 84 cells that displayed clear deformation of the nuclear membrane in a single optical plane during a 4–8-min time period. 81 cells (~96%) showed that the deformation of the nuclear membrane was clearly due to a pushing mechanism (Table III). The mechanism was ambiguous in the remaining three cells because MTs were touching the cell tip in both directions. No instances of nuclear pulling were observed. In all 84 cells, the nucleus only moved when the MT reached the cell tip. In all 84 cells (100%), the medial-bundled MT region overlapped with the functional nuclear attachment site. Thus, this pushing mechanism is used to move the nucleus in the vast majority of interphase fission yeast cells.

Table III. Interphase MTs Push on the Nucleus in S. pombe

Cells with clear deformation of nucleus	84
Cells with MT pushing force	81
Cells with MT pulling force	0
Ambiguous	3
Cells with functional nuclear attachment zone in MT overlap region	84

127 interphase cells (PT.65) expressing nup107-GFP and GFP-tubulin were imaged at 5-s intervals for 4–8 min in a single optical plane using confocal microscopy. Analysis of these time-lapse sequences revealed that 84 cells exhibited a clear deformation of the nucleus within this time period in this focal plane. Analysis of MTs during the deformation event was used to determine the type of force involved in deformation. MT pushing force was defined as MT contacting the cell tip, elongating, and producing a pushing force on the nuclear envelope away from the contacted cell tip; the opposite MT in the bundle was not contacting the cell tip. MT pulling force was defined as an MT contacting the cell tip and shortening and producing a pulling force on the nuclear envelope towards the contracted cell tip. Ambiguous force was defined in circumstances where MTs contacted both cell tips during deformation. In all cases examined, the MT overlap region was contiguous with the nuclear envelope and moved with the deformed nuclear envelope, suggesting the presence of a functional nuclear attachment site within the central MT overlap region.

A Computer Model for Nuclear Positioning

Our experimental results suggested a model for nuclear positioning based on simple MT pushing forces. To test if this simple model is sufficient to explain proper centering of the nucleus, we generated an iterative algorithm of this process (see Materials and Methods). The inputs were parameters of MT dynamics and organization as measured in this paper, with the nucleus having one or more bundle of leftward and rightward pairs of dynamic MTs attached to and pushing on the nucleus; the output from the algorithm was nuclear position. In the computer simulation, dynamic MTs were capable of centering an offset nucleus by a pushing mechanism. Starting at the left tip of the cell at time 0, a nucleus with one MT bundle moved towards a medial position after ~10 min and then oscillated around the medial position (Fig. 9 A). In multiple simulations, 50% of nuclei were located within 10% of the cell length away from the medial position (Fig. 9 B). We also tested various parameters using this computer model. If the nucleus was attached to four MT bundles, the nucleus was more stable and exhibited less oscillatory deviation than a nucleus with one attached MT bundle (Fig. 9 B). To test if symmetry of MTs was important for centering, nuclei with two MTs on the left and one MT on the right were tested. The average positions of nuclei with asymmetric MTs were skewed toward the side with only one MT (Fig. 9 B). Thus, the best nuclear centering resulted from multiple attached MTs with equal numbers of MTs on each side of the nucleus. The amplitude of oscillation and deviation was greater in the computer simulation than observed in vivo, suggesting that additional forces in the cell, such as viscosity or membrane tension, may also exert effects on nuclear po-

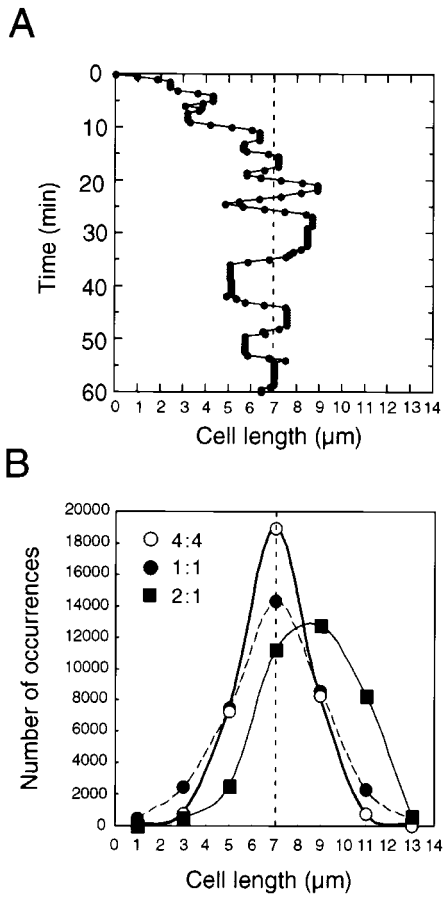

Figure 9. Nuclear positioning in a computer-modeled cell. (A) Position of computer-modeled cell nucleus after release from a cell end. Nuclear position was calculated by computer based on an algorithm in which nuclear movement was solely dependent on MT pushing forces using parameters seen in living cells (see Materials and Methods). For a 14-μm cell with one antiparallel MT pair, the position of the nucleus was recorded every 30 s for a modeled period of 1 h. (B) Distribution of observed nuclear positions with different MT arrangements. Nuclear position was recorded at 1-s intervals for 1 h for 10 modeled cells for each MT arrangement. The nucleus of each cell was initially at the center of the 14-μm cell. The sum of total observed occurrences of nuclei within specified spatial intervals is reported: (●) 1 left MT, 1 right MT; (○) 4 left MTs, 4 right MTs; (■) 2 left MTs, 1 right MT.

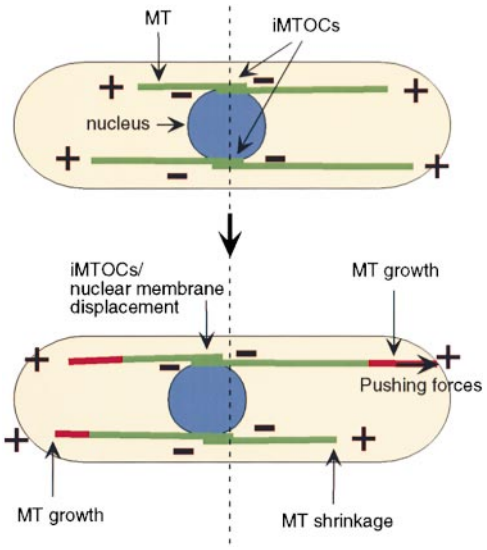

Figure 10. A model for nuclear positioning and interphase MT architecture in *S. pombe*. MTs are organized from medial organizing centers (iMTOCs) in multiple bundles with an antiparallel configuration and dynamic plus ends facing the cell tips and minus ends in medial-bundled regions. One MT bundle is attached to the nuclear envelope at the SPB, and other MT bundles may be attached at additional sites. When an MT end contacts the cell tip, MT polymerization produces a transient pushing force that pushes the MT lattice and attached nucleus away from that cell tip. A balance of these pushing forces from these MTs may position the nucleus in the middle of the cell.

sitioning. Addition of a conservative term for viscosity further improved centering (Marsh, L., unpublished observations). Nevertheless, these results show that a simple mechanism based upon MT pushing is sufficient to center the nucleus.

Discussion

Here, our studies have defined a novel mechanism for how the nucleus is positioned by MTs at the middle of the fission yeast cell (Fig. 10). Key parameters include: (a) organization of MTs in three to four bundles in an antiparallel configuration, with the plus ends facing the cell tips and the minus ends near the middle of the cell; (b) regulated MT dynamics so that MT plus ends exhibit catastrophe 1.5 min after contacting the cell tip; and (c) transient MT pushing forces on the nuclear envelope when MT plus ends contact the cell tip so that MT ends are constantly sensing the position of the cell tips. A computer model shows that a mechanism based on these parameters can indeed center the nucleus. These studies illustrate how dynamic MTs can provide a way for a cell to measure distances, sense cell size, and define its middle.

MT Organization in Interphase S. pombe Cells

Our analysis of living *S. pombe* cells using GFP-tubulin showed that the interphase MT cytoskeleton (at 23–25°C) consists of three to four MT bundles that extend the length of the cell. These numbers of bundles are consistent with measurements by Yamamoto et al. (1999) but are fewer than those observed by Paluh et al. (2000), possibly because of differences in temperature or sample preparation. Fluorescence intensity and MT dynamics suggest that each MT bundle may contain single MTs at the cell tips and two to three MTs at the medial-bundled region. Electron micrographs show single or bundles of cytoplasmic MTs (Hereward, 1974; Streiblova and Girbardt, 1980; Kanbe et al., 1989; Ding et al., 1997), but since MTs are not well preserved, EM data illustrating this arrangement have not yet been obtained. Although we have assumed this arrangement for discussion, we cannot rule out the formal possibility that these bundles have many more MTs in the bundle, although this would require that multiple MTs display dynamics that are somehow coordinated. Analysis of MT dynamics and fluorescence speckles suggests that the plus ends of MTs face the cell tips and the minus ends are near

the middle of the cell, with most of the growth and shrinkage of the MT occurring at the plus ends (Fig. 10). An MT grows to the cell tip, continues to grow for 1.5 min, and then exhibits catastrophe when it shrinks back to the medial region. Depending on cell length, an MT from each bundle may reach the tip every 4–6 min.

At the middle of each MT bundle is a region of bundled antiparallel MTs, which is stable to depolymerization. MTs grew from and shrank to these regions but did not shrink past these regions. MT depolymerization revealed two to four discrete dots of stable MTs near the nuclear envelope. Each dot was capable of regrowing into an MT bundle and was located within the larger bundled region of each MT bundle. We have termed these regions interphase MTOCs (iMTOCs), since they appear to organize the interphase MT cytoskeleton.

Although we have described the most common MT organization, more complicated MT behaviors, such as release of free nonbundled MTs and dynamics of MTs within bundles, were occasionally seen (our unpublished observations). However, these other behaviors do not appear to contribute generally to the mechanism of nuclear positioning.

While this paper was in revision, a similar paper describing *S. pombe* interphase MT organization and dynamics was published (Drummond and Cross, 2000). Their general conclusions of MTs being arranged in antiparallel bundles agreed with this study, although some of the rates of MT dynamics were different. These differences may be due to differences in strain and GFP-tubulin fusion used, their much smaller sample size, and significant differences in the methods of imaging and analysis of dynamics.

MT Forces on the Nucleus

MTs are required for accurate nuclear positioning at the middle of the cell. Our data showed that MTs are responsible for exerting frequent, small, transient pushing forces on the nuclear envelope (Fig. 10). The SPB is associated with some of the deformities of the nuclear envelope, showing that it is a major site of MT attachment to the nucleus (Fig. 6). However, there are clearly additional effects of MTs on the nuclear envelope that are spatially distinct from the SPB, suggesting the presence of additional MT attachment sites. These additional sites are associated with minor dots of sad1-GFP when this fusion is overexpressed (Fig. 6). The MT bundles are attached or associated with the nuclear envelope within the medial MT-bundled regions (Table III). At least some of the interphase MT bundles are not attached to the nucleus, and some attachments may even be transient (our unpublished observations); thus, future studies will be needed to characterize the nature of these MT attachments further.

By examining the effects of individual MT bundles on the nucleus, we determined that MTs exert primarily pushing forces on the nucleus. The nucleus moved away from the cell tip only when an MT contacted and continued to grow at the cell tip. The rate of movement of the nuclear envelope matched the rate of MT polymerization at the cell tip, the movement of the MT lattice, and the movement of the medial MT-bundled region. They all moved at rates of 1–2 μm min^{-1} and exhibited excursions of 1–3 μm (Figs. 2, 3, 5, 7, and 8). Buckling of the MT further indicated pushing forces between the cell tip and nucleus. Our observations showed no nuclear movements consistent with pulling, tracking, or sliding mechanisms, although we do not rule out that other types of forces may provide minor contributions. Although MT pushing forces have been shown to center a centrosome in vitro in a round well (Holy et al., 1997), these studies establish a novel MT pushing mechanism for centering the nucleus in vivo.

This MT pushing force may arise from simple MT polymerization, since the rate of nuclear movement generally correlated with the rate of MT polymerization. Forces from the polymerization of a single MT can theoretically supply enough force (3–4 pN) (Dogterom and Yurke, 1997) to move a nucleus, and thus motor proteins may not be necessary for force generation. However, it is formally possible that an MT motor protein (plus-ended motor) anchored at the cell tip may contribute pushing forces as well. Motor proteins may also play roles in regulating MT dynamics. Mutations in the *S. pombe* MT motor proteins plk1, klp3, and dynein have not been reported to produce a nuclear positioning defect (Pidoux et al., 1996; Yamamoto et al., 1999; Brazer et al., 2000). The Kip2-like kinesin tea2p is located at cell tips and often at MT ends, but its role in nuclear positioning is not yet clear, since *tea2* mutant cells have defects in MT stability and exhibit short MTs that do not extend to the cell tips (Verde et al., 1995; Browning et al., 2000).

Our findings suggest a mechanism for how the nucleus is positioned at the middle of the cell. The symmetry in MT arrangement produces a ready balance of forces that may center the nucleus between the two cell tips. An offset nucleus would encounter more frequent pushing forces from MTs from the side closest to the cell tip, since MTs would reach the closer cell tip more often due to the shorter distance to travel. The amount of pushing force exerted by an MT is also dependent on its length. Longer MTs are less rigid than short ones and buckle under a pushing force more readily than short ones. Thus, short MTs are more effective than long MTs in pushing the nucleus or in resisting forces from opposing MTs. For example, in a 14-μm-long cell with an offset nucleus, a 4-μm MT on one side would have a critical buckling force of $F_c = \pi^2 EI/L^2 \approx 15$ pN, whereas the 10-μm MT on the opposite side would have $F_c \approx 2$ pN (the flexural rigidity, EI, of an MT is assumed to be 25×10^{-24} Nm^2) (Mickey and Howard, 1995; Felgner et al., 1997).

The results of a computer model that used the parameters observed in this paper suggest that this simple MT pushing model may, in fact, be largely sufficient to center the nucleus (Fig. 9). Even with deliberately parsimonious parameters and a nonoptimized algorithm, the simulated MTs were able to center an offcentered nucleus and maintain its centered position. As the nucleus in the computer simulation exhibited greater oscillations than those seen in vivo, it is likely that there are additional minor forces that further restrict these oscillations. These factors may include viscosity, nuclear envelope tension and attachments, the actin cytoskeleton, and modulations of MT dynamics. It will be interesting to compare the effects of varying various parameters on nuclear positioning in vivo and the computer model.

We envision that iMTOCs contain several activities, including MT bundling and stabilizing factors and perhaps nuclear attachment factors. In its simplest form, an

iMTOC would contain a pair of MTs bundled together in an antiparallel arrangement, so that it sends MTs in two opposite directions and not in an aster arrangement (Figs. 1–4, 7, and 8). Although the iMTOC may function in some respects as an MTOC, we have no evidence that it may nucleate MTs de novo, and γ-tubulin has not been reported to be in these multiple medial dots (Horio et al., 1999; Paluh et al., 2000). The SPB intersects one of the MT bundles and thus, may represent one of the iMTOCs or be adjacent to an iMTOC. Whether the SPB continues to nucleate cytoplasmic MTs through interphase is still not clear and has not been addressed in this study. Although no proteins at endogenous levels other than tubulin have been localized to the iMTOC structures, a candidate component is sad1p. Mild overexpression of sad1-GFP led to the visualization of minor sad1-GFP dots that were associated with sites of nuclear membrane deformations. Thus, sad1 may be a component of the MT nuclear attachment site or associate with the site when overexpressed.

An important parameter in this arrangement is the amount of time an MT pushes at the tip. MTs continue to grow at the tip for 1.5 min before catastrophe. At an MT growth rate of 1–2 μm min^{-1}, this period would result in 1–3-μm displacement of the nucleus (including some rotation). This timing is crucial for the whole mechanism, since too short or too long of a period would cause not enough or too much displacement of the nucleus, respectively. It is unlikely that this catastrophe is induced merely by contacting any plasma membrane, since the MTs that touch the sides (nontip region) of the cells continue growing (Fig. 4 C). We propose that there is a catastrophe-inducing factor located at both tips of the cell that will induce catastrophe 1.5 min after the MT contacts the tip. An alternative model is that MT growth at cell tips generates stall forces that lead to MT catastrophe. This property provides a mechanism for orienting MTs along the longitudinal axis of the cell. Mutations in some polarity factors (Verde et al., 1995) and mutations that stabilized MTs (Paluh et al., 2000) lead to MTs that do not stop growing at the cell tip but wrap around the cell ends and cause loss of cell polarity and proper nuclear positioning. A recent study on a CLIP170-like protein tip1p suggests that MTs may be stabilized by a plus-end cap that is removed at the cell tip (Brunner and Nurse, 2000). Thus, MT regulation at the cell tip may be critical for regulating the position of the nucleus at the middle of the cell.

One important caveat to these studies is the use of GFP-tubulin as a marker. Although GFP-atb2p certainly incorporates into MTs, it has not been shown to be functional and thus potentially could perturb function. We cannot rule out that GFP-atb2p may alter the properties of MTs in some subtle way. However, numerous lines of evidence suggest that the GFP-atb2p does not affect MT organization or function in a significant manner. (a) Cells expressing GFP-atb2 have no detectable phenotype in terms of cell cycle, cell shape, mitosis, MT organization, or nuclear distribution. (b) MTs in cells expressing different amounts of GFP-tubulin exhibit similar dynamics and MT organization (Table I). (c) At low expression levels, cells that exhibit speckling may only have 1–5% of the tubulin in the MT lattice as GFP-tubulin (Waterman-Storer and Salmon, 1998; Waterman-Storer et al., 1998). (d) SPB dynamics, which were measured without GFP-tubulin, were consistent with MT dynamics. (e) Finally, we find it highly unlikely that an entirely different mechanism of nuclear positioning would be created by expression of this GFP fusion protein.

Nuclear Positioning throughout the Life Cycle

Here, we have focused on MTs and nuclear positioning in the interphase cells during vegetative growth. However, MT organization and mechanisms of nuclear positioning clearly vary during the *S. pombe* life cycle (Hagan, 1998). During mitosis, the interphase MTs disappear and the SPBs organize the mitotic spindle inside the nucleus. After anaphase, the two nuclei move from the cell tips inward toward the center of each new daughter cell (Hagan and Hyams, 1988). Although it has been proposed that these nuclei may be pulled to the middle of the cell (Hagan and Yanagida, 1997), pushing forces may be involved in centering the nucleus even at this early stage (our unpublished observations). During conjugation, the nucleus moves to the projection tip where a new conjugation-specific MTOC aster is formed (Petersen et al., 1998). During meiotic prophase, the nucleus undergoes MT-dependent nuclear oscillation (horse tail movement), which appears to facilitate recombination (Ding et al., 1998; Yamamoto et al., 1999). The entire organization of the MTs changes; most of the MTs emanate from the SPB in an astral pattern. In contrast to interphase nuclear positioning, meiotic nuclear movement is dynein dependent and may proceed using a pulling mechanism from either the cell tip or SPB (Yamamoto et al., 1999). It will be interesting to examine how different components responsible for these programs in nuclear positioning are differently regulated during these various phases of the cell cycle.

Spatial Requirements in a Cylindrical Cell

This arrangement of MTs and the nucleus establishes a cellular axis that regulates other aspects of spatial regulation in the cell. The nucleus needs to be positioned in the middle of the cell because the nucleus may specify the future site of cell division through proteins such as mid1p (Chang and Nurse, 1996; Paoletti and Chang, 2000; Tran et al., 2000). MT plus ends need to be facing the cell tips to regulate the establishment of cell-polarized growth at the cell tips through proteins such as tea1p (Mata and Nurse, 1997). One reason why fission yeast may use this mechanism is because it represents a reliable and stable arrangement for positioning the nucleus and MT plus ends in a cylindrical cell. A radial MT arrangement may work in a round cell but may not be optimal for a cylindrical cell. For instance, we have characterized a fission yeast mutant (*rsp1*) that lacks the bundled MTs and exhibits MTs organized in a more radial arrangement. This mutant has a severe defect in nuclear positioning (Tran, P., O. Niwa, and F. Chang, unpublished observations). It will be interesting to see if other cell types, perhaps with elongated cell shapes, also use this arrangement of multiple bundled MTs. For instance, multiple MTOCs have been found on the nucleus in some plant cells and in myocytes (Tassin et al., 1985; Baluska et al., 1997).

We thank Drs. D.-Q. Ding and Y. Hiraoka for their kind gift of the pDQ105 plasmid; Drs. G. Goshima and M. Yanagida for the pTN501 plasmid; and Dr. T. Davis for her gift of the GFP-cmd1 strain. V. Doye thanks P. Philippsen for his generous gift of the pFA6a-GFP-kanMX6 plasmid and N. Rossignol for his technical assistance. S. Inoue thanks Yokogawa Electric Corp. for use of the CSU-10 real-time confocal scanner. P. Tran thanks P. Maddox (University of North Carolina) for his expert advice on the use of MetaMorph. We thank Dr. H. Rey (Nikon), B. Semon (Morrell Inc.), L. Hamilton and S. Randall (Improvision Corp.), and D. Bowman (Universal Imaging Corp.) for instrument supports. We are grateful to Drs. E.D. Salmon (University of North Carolina), L. Pon (Columbia University), A. Paoletti (Institut Curie), M. Smith, I. Boldogh, H.-C. Yang, and B. Feierbach, and J. Glynn, A. Berlin, R. Lustig, S. Kaplan, and K. Fehrenbacher (Columbia University) for their helpful comments.

P. Tran was supported by a National Institutes of Health postdoctoral fellowship. V. Doye was supported by the Centre National de la Recherche Scientifique (UMR144), the Institut Curie, and a grant from the Association pour la Recherche contre le Cancer. F. Chang was supported by grants from the National Institutes of Health (R01-GM5-35540), March of Dimes Basil O'Conner Starter Scholar Award, the Irma T. Hirschl Foundation, and a grant from the Howard Hughes Medical Institute to Columbia University for new investigators.

Submitted: 7 December 2000
Revised: 9 February 2001
Accepted: 14 February 2001

References

Adames, N.R., and J.A. Cooper. 2000. Microtubule interactions with the cell cortex causing nuclear movements in *Saccharomyces cerevisiae*. *J. Cell Biol*. 149:863–874.

Bahler, J., J.Q. Wu, M.S. Longtine, N.G. Shah, A. McKenzie III, A.B. Steever, A. Wach, P. Philippsen, and J.R. Pringle. 1998. Heterologous modules for efficient and versatile PCR-based gene targeting in *Schizosaccharomyces pombe*. *Yeast*. 14:943–951.

Baluska, F., D. Volkmann, and P.W. Barlow. 1997. Nuclear components with microtubule-organizing properties in multicellular eukaryotes: functional and evolutionary considerations. *Int. Rev. Cytol*. 175:91–135.

Beinhauer, J.D., I.M. Hagan, J.H. Hegemann, and U. Fleig. 1997. Mal3, the fission yeast homologue of the human APC-interacting protein EB-1 is required for microtubule integrity and the maintenance of cell form. *J. Cell Biol.* 139:717–728.

Bezanilla, M., J.M. Wilson, and T.D. Pollard. 2000. Fission yeast myosin-II isoforms assemble into contractile rings at distinct times during mitosis. *Curr. Biol*. 10:397–400.

Brazer, S.C., H.P. Williams, T.G. Chappell, and W.Z. Cande. 2000. A fission yeast kinesin affects Golgi membrane recycling. *Yeast.* 16:149–166.

Browning, H., J. Hayles, J. Mata, L. Aveline, P. Nurse, and J.R. McIntosh. 2000. Tea2p is a kinesin-like protein required to generate polarized growth in fission yeast. *J. Cell Biol.* 151:15–28.

Brunner, D., and P. Nurse. 2000. CLIP170-like tip1p spatially organizes microtubular dynamics in fission yeast. *Cell.* 102:695–704.

Carminati, J.L., and T. Stearns. 1997. Microtubules orient the mitotic spindle in yeast through dynein-dependent interactions with the cell cortex. *J. Cell Biol*. 138:629–641.

Chang, F. 1999. Movement of a cytokinesis factor cdc12p to the site of cell division. *Curr. Biol*. 9:849–852.

Chang, F., and P. Nurse. 1996. How fission yeast fission in the middle. *Cell*. 84: 191–194.

Chen, C.R., Y.C. Li, J. Chen, M.C. Hou, P. Papadaki, and E.C. Chang. 1999. Moe1, a conserved protein in *Schizosaccharomyces pombe*, interacts with a Ras effector, Scd1, to affect proper spindle formation. *Proc. Natl. Acad. Sci. USA*. 96:517–522.

Desai, A., and T.J. Mitchison. 1997. Microtubule polymerization dynamics. *Annu. Rev. Cell Dev. Biol*. 13:83–117.

Ding, D.Q., Y. Chikashige, T. Haraguchi, and Y. Hiraoka. 1998. Oscillatory nuclear movement in fission yeast meiotic prophase is driven by astral microtubules, as revealed by continuous observation of chromosomes and microtubules in living cells. *J. Cell Sci*. 111:701–712.

Ding, R., R.R. West, D.M. Morphew, B.R. Oakley, and J.R. McIntosh. 1997. The spindle pole body of *Schizosaccharomyces pombe* enters and leaves the nuclear envelope as the cell cycle proceeds. *Mol. Biol. Cell*. 8:1461–1479.

Dogterom, M., and B. Yurke. 1997. Measurement of the force-velocity relation for growing microtubules. *Science*. 278:856–860.

Drummond, D.R., and R.A. Cross. 2000. Dynamics of interphase microtubules in *Schizosaccharomyces pombe*. *Curr. Biol*. 10:766–775.

Felgner, H., R. Frank, J. Biernat, E.M. Mandelkow, E. Mandelkow, B. Ludin, A. Matus, and M. Schliwa. 1997. Domains of neuronal microtubule-associated proteins and flexural rigidity of microtubules. *J. Cell Biol*. 138:1067–1075.

Gildersleeve, R.F., A.R. Cross, K.E. Cullen, A.P. Fagen, and R.C. Williams, Jr. 1992. Microtubules grow and shorten at intrinsically variable rates. *J. Biol. Chem*. 267:7995–8006.

Gonczy, P., S. Pichler, M. Kirkham, and A.A. Hyman. 1999. Cytoplasmic dynein is required for distinct aspects of MTOC positioning, including centrosome separation, in the one cell stage *Caenorhabditis elegans* embryo. *J. Cell Biol*. 147:135–150.

Goshima, G., S. Saitoh, and M. Yanagida. 1999. Proper metaphase spindle length is determined by centromere proteins Mis12 and Mis6 required for faithful chromosome segregation. *Genes Dev*. 13:1664–1677.

Hagan, I., and M. Yanagida. 1995. The product of the spindle formation gene sad1+ associates with the fission yeast spindle pole body and is essential for viability. *J. Cell Biol*. 129:1033–1047.

Hagan, I., and M. Yanagida. 1997. Evidence for cell cycle-specific, spindle pole body-mediated, nuclear positioning in the fission yeast *Schizosaccharomyces pombe*. *J. Cell Sci*. 110:1851–1866.

Hagan, I.M. 1998. The fission yeast microtubule cytoskeleton. *J. Cell Sci*. 111: 1603–1612.

Hagan, I.M., and J.S. Hyams. 1988. The use of cell division cycle mutants to investigate the control of microtubule distribution in the fission yeast *Schizosaccharomyces pombe*. *J. Cell Sci*. 89:343–357.

Hagan, I.M., P.N. Riddle, and J.S. Hyams. 1990. Intramitotic controls in the fission yeast *Schizosaccharomyces pombe*—the effect of cell size on spindle length and the timing of mitotic events. *J. Cell Biol*. 110:1617–1621.

Hereward, F.V. 1974. Rough membranes in *Schizosaccharomyces pombe* protoplasts. *Exp. Cell Res.* 87:213–218.

Holy, T.E., M. Dogterom, B. Yurke, and S. Leibler. 1997. Assembly and positioning of microtubule asters in microfabricated chambers. *Proc. Natl. Acad. Sci. USA*. 94:6228–6231.

Horio, T., and H. Hotani. 1986. Visualization of the dynamic instability of individual microtubules by dark-field microscopy. *Nature*. 321:605–607.

Horio, T., A. Basaki, A. Takeoka, and M. Yamato. 1999. Lethal level overexpression of gamma-tubulin in fission yeast causes mitotic arrest. *Cell Motil. Cytoskeleton*. 44:284–295.

Inoué, S., and E.D. Salmon. 1995. Force generation by microtubule assembly/disassembly in mitosis and related movements. *Mol. Biol. Cell*. 6:1619–1640.

Kanbe, T., I. Kobayashi, and K. Tanaka. 1989. Dynamics of cytoplasmic organelles in the cell cycle of the fission yeast *Schizosaccharomyces pombe*: three-dimensional reconstruction from serial sections. *J. Cell Sci*. 94:647–656.

Koonce, M.P., J. Kohler, R. Neujahr, J.M. Schwartz, I. Tikhonenko, and G. Gerisch. 1999. Dynein motor regulation stabilizes interphase microtubule arrays and determines centrosome position. *EMBO (Eur. Mol. Biol. Organ.) J*. 18:6786–6792.

Maddox, P.S., K.S. Bloom, and E.D. Salmon. 2000. The polarity and dynamics of microtubule assembly in the budding yeast *Saccharomyces cerevisiae*. *Nat. Cell Biol*. 2:36–41.

Mata, J., and P. Nurse. 1997. tea1 and the microtubular cytoskeleton are important for generating global spatial order within the fission yeast cell. *Cell*. 89: 939–949.

Mickey, B., and J. Howard. 1995. Rigidity of microtubules is increased by stabilizing agents. *J. Cell Biol*. 130:909–917.

Mitchison, J.M., and P. Nurse. 1985. Growth in cell length in the fission yeast *Schizosaccharomyces pombe*. *J. Cell Sci*. 75:357–376.

Moser, M.J., M.R. Flory, and T.N. Davis. 1997. Calmodulin localizes to the spindle pole body of *Schizosaccharomyces pombe* and performs an essential function in chromosome segregation. *J. Cell Sci*. 110:1805–1812.

Nurse, P. 1994. Fission yeast morphogenesis—posing the problems. *Mol. Biol. Cell*. 5:613–616.

Paluh, J.L., E. Nogales, B.R. Oakley, K. McDonald, A.L. Pidoux, and W.Z. Cande. 2000. A mutation in gamma-tubulin alters microtubule dynamics and organization and is synthetically lethal with the kinesin-like protein pkl1p. *Mol. Biol. Cell*. 11:1225–1239.

Paoletti, A., and F. Chang. 2000. Analysis of mid1p, a protein required for placement of the cell division site, reveals a link between the nucleus and the cell surface in fission yeast. *Mol. Biol. Cell.* 11:2757–2773.

Petersen, J., M.J. Heitz, and I.M. Hagan. 1998. Conjugation in *S. pombe*: identification of a microtubule-organising centre, a requirement for microtubules and a role for Mad2. *Curr. Biol*. 8:963–966.

Pidoux, A.L., M. LeDizet, and W.Z. Cande. 1996. Fission yeast pkl1 is a kinesin-related protein involved in mitotic spindle function. *Mol. Biol. Cell*. 7:1639–1655.

Plamann, M., P.F. Minke, J.H. Tinsley, and K.S. Bruno. 1994. Cytoplasmic dynein and actin-related protein Arp1 are required for normal nuclear distribution in filamentous fungi. *J. Cell Biol*. 127:139–149.

Radcliffe, P., D. Hirata, D. Childs, L. Vardy, and T. Toda. 1998. Identification of novel temperature-sensitive lethal alleles in essential beta-tubulin and nonessential alpha 2-tubulin genes as fission yeast polarity mutants. *Mol. Biol. Cell*. 9:1757–1771.

Radu, A., G. Blobel, and R.W. Wozniak. 1994. Nup107 is a novel nuclear pore complex protein that contains a leucine zipper. *J. Biol. Chem*. 269:17600–17605.

Reinsch, S., and P. Gonczy. 1998. Mechanisms of nuclear positioning. *J. Cell*

Sci. 111:2283–2295.

Robinson, J.T., E.J. Wojcik, M.A. Sanders, M. McGrail, and T.S. Hays. 1999. Cytoplasmic dynein is required for the nuclear attachment and migration of centrosomes during mitosis in *Drosophila*. *J. Cell Biol.* 146:597–608.

Sawin, K.E., and P. Nurse. 1998. Regulation of cell polarity by microtubules in fission yeast. *J. Cell Biol.* 142:457–471.

Shaw, S.L., E. Yeh, P. Maddox, E.D. Salmon, and K. Bloom. 1997. Astral microtubule dynamics in yeast: a microtubule-based searching mechanism for spindle orientation and nuclear migration into the bud. *J. Cell Biol.* 139:985–994.

Siniossoglou, S., C. Wimmer, M. Rieger, V. Doye, H. Tekotte, C. Weise, S. Emig, A. Segref, and E.C. Hurt. 1996. A novel complex of nucleoporins, which includes Sec13p and a Sec13p homolog, is essential for normal nuclear pores. *Cell.* 84:265–275.

Streiblova, E., and M. Girbardt. 1980. Microfilaments and cytoplasmic microtubules in cell division cycle mutants of *Schizosaccharomyces pombe. Can. J. Microbiol.* 26:250–254.

Tassin, A.M., B. Maro, and M. Bornens. 1985. Fate of microtubule-organizing centers during myogenesis in vitro. *J. Cell Biol.* 100:35–46.

Toda, T., K. Umesono, A. Hirata, and M. Yanagida. 1983. Cold-sensitive nuclear division arrest mutants of the fission yeast *Schizosaccharomyces pombe*. *J. Mol. Biol.* 168:251–270.

Tran, P.T., P. Maddox, F. Chang, and S. Inoue. 1999. Dynamic confocal imaging of interphase and mitotic microtubules in the fission yeast, *S. pombe*. *Biol. Bull.* 197:262–263.

Tran, P.T., V. Doye, F. Chang, and S. Inoue. 2000. Microtubule-dependent nuclear positioning and nuclear-dependent septum positioning in the fission yeast *S. pombe*. *Biol. Bull.* 199:205–206.

Umesono, K., T. Toda, S. Hayashi, and M. Yanagida. 1983. Cell division cycle genes nda2 and nda3 of the fission yeast *Schizosaccharomyces pombe* control microtubular organization and sensitivity to anti-mitotic benzimidazole compounds. *J. Mol. Biol.* 168:271–284.

Verde, F., M. Dogterom, E. Stelzer, E. Karsenti, and S. Leibler. 1992. Control of microtubule dynamics and length by cyclin A– and cyclin B–dependent kinases in *Xenopus* egg extracts. *J. Cell Biol.* 118:1097–1108.

Verde, F., J. Mata, and P. Nurse. 1995. Fission yeast cell morphogenesis: identification of new genes and analysis of their role during the cell cycle. *J. Cell Biol.* 131:1529–1538.

Wach, A., A. Brachat, C. Alberti-Segui, C. Rebischung, and P. Philippsen. 1997. Heterologous HIS3 marker and GFP reporter modules for PCR-targeting in *Saccharomyces cerevisiae*. *Yeast.* 13:1065–1075.

Walker, G.M. 1982. Cell cycle specificity of certain antimicrotubular drugs in *Schizosaccharomyces pombe*. *J. Gen. Microbiol.* 128:61–71.

Walker, R.A., E.T. O'Brien, N.K. Pryer, M.F. Soboeiro, W.A. Voter, H.P. Erickson, and E.D. Salmon. 1988. Dynamic instability of individual microtubules analyzed by video light microscopy: rate constants and transition frequencies. *J. Cell Biol.* 107:1437–1448.

Waterman-Storer, C.M., and E.D. Salmon. 1998. How microtubules get fluorescent speckles. *Biophys. J.* 75:2059–2069.

Waterman-Storer, C.M., A. Desai, J.C. Bulinski, and E.D. Salmon. 1998. Fluorescent speckle microscopy, a method to visualize the dynamics of protein assemblies in living cells. *Curr. Biol.* 8:1227–1230.

Xiang, X., S.M. Beckwith, and N.R. Morris. 1994. Cytoplasmic dynein is involved in nuclear migration in *Aspergillus nidulans*. *Proc. Natl. Acad. Sci. USA*. 91:2100–2104.

Yamamoto, A., R.R. West, J.R. McIntosh, and Y. Hiraoka. 1999. A cytoplasmic dynein heavy chain is required for oscillatory nuclear movement of meiotic prophase and efficient meiotic recombination in fission yeast. *J. Cell Biol.* 145:1233–1249.

Yeh, E., R.V. Skibbens, J.W. Cheng, E.D. Salmon, and K. Bloom. 1995. Spindle dynamics and cell cycle regulation of dynein in the budding yeast, *Saccharomyces cerevisiae*. *J. Cell Biol.* 130:687–700.